JAERI-Research
97-088

MEASUREMENT OF REACTIVITY WORTHS OF SM, CS, GD, ND, RH, EU, B AND ER AQUEOUS SOLUTION SAMPLES

November 1997

Yuichi KOMURO, Takenori SUZAKI, Shoichi OHTOMO*
Kiyoshi SAKURAI and Oichiro HORIKI

日本原子力研究所
Japan Atomic Energy Research Institute

本レポートは，日本原子力研究所が不定期に公刊している研究報告書です。
入手の問合わせは，日本原子力研究所研究情報部研究情報課（〒319-11 茨城県那珂郡東海村）あて，お申し越しください。なお，このほかに財団法人原子力弘済会資料センター（〒319-11 茨城県那珂郡東海村日本原子力研究所内）で複写による実費頒布をおこなっております。

This report is issued irregularly.
Inquiries about availability of the reports should be addressed to Research Information Division, Department of Intellectual Resources, Japan Atomic Energy Research Institute, Tokai-mura, Naka-gun, Ibaraki-ken 319-11, Japan.

編集兼発行　日本原子力研究所
印　　刷　㈱原子力資料サービス

Measurement of Reactivity Worths of Sm, Cs, Gd, Nd, Rh, Eu, B and Er Aqueous Solution Samples

Yuichi KOMURO, Takenori SUZAKI[+1], Shoichi OHTOMO*
Kiyoshi SAKURAI[+2] and Oichiro HORIKI[+3]

Department of Research Reactor
Tokai Research Establishment
Japan Atomic Energy Research Institute
Tokai-mura, Naka-gun, Ibaraki-ken

(Received October 28, 1997)

From the view point of burnup credit for spent fuels, it remains as an important issue to validate nuclear data of fission products. Aiming to obtain benchmark data for that purpose, reactivity worths of Sm, Cs, Gd, Nd, Rh and Eu aqueous solution samples of various concentrations were measured by the critical-water-level method at Tank-type Critical Assembly (TCA). Samples of B and Er were included for the purpose of comparison. Neutron activation distributions of Au wires crossing the sample region were also measured in several cases. A linear correlation was found between the thermal neutron flux peakings in the sample region and the reactivity worths.

Keywords: Critical Experiment, Criticality Data, Burnup Credit, Fission Product, Samarium, Cesium, Gadolinium, Neodymium, Rhodium, Europium, Boron, Aqueous Solution Sample, Reactivity Worths, Activation Distribution, TCA

+1 Department of Fuel Cycle Safety Research
+2 Nuclear Safety Research Center
+3 Tokai Education Center, Nuclear Technology and Education Center
* Radiation Application Development Measurement Association

Sm, Cs, Gd, Nd, Rh, Eu, B及びEr水溶液試料の反応度価値の測定

日本原子力研究所東海研究所研究炉部
小室　雄一　・須崎　武則[+1]・大友　正一*
桜井　　淳[+2]・堀木欧一郎[+3]

（1997年10月28日受理）

使用済燃料の燃焼度クレジットの観点から、核分裂生成物の核データを検証することは重要な課題として残されている。そのための検証用データを得るために、タンク型臨界集合体（TCA）を用いてSm, Cs, Gd, Nd, Rh及びEuの各種濃度の水溶液試料の反応度価値を臨界水位法により測定した。比較のため、B及びErの試料も実験に供された。いくつかのケースについては、試料領域を横切って据え付けた金線の中性子放射化率分布を測定した。試料領域中の熱中性子束のピーキングと反応度価値の間には直線関係が見出された。

東海研究所：〒319-11　茨城県那珂郡東海村白方白根2-4
+1 安全性試験研究センター燃料サイクル安全工学部
+2 安全性試験研究センター
+3 国際原子力総合技術センター東海研修センター
*（財）放射線利用振興協会

Contents

目　　次

1. Introduction

In the past, criticality safety assessments for a system containing spent fuel were usually performed on the assumption that all the fuel was fresh. Although this assumption requires no burnup calculation process for the composition of the spent fuel, it may result in a considerable economic burden on the nuclear facility operation. To obtain economic improvement, a new approach based on burnup credit has recently been introduced into the assessment. The reduction in fuel reactivity occurring with burnup, due to the depletion of the fissile nuclide and the build-up of fission products and higher actinides, is taken into account by the approach. The twelve fission products listed in Table 1 were identified as the most important isotopes for burnup credit calculations.[1]

The main objective of the experiments described in this paper is to provide criticality data that can be used to validate nuclear data for some isotopes listed in Table 1. This validation is an important activity for the concept of taking advantage of burnup of fuel for criticality safety assessment. A similar experiment was carried out in France[2].

The following nitrate compounds were used in our experiments :

$Sm(NO_3)_3$, $CsNO_3$, $Gd(NO_3)_3$, $Nd(NO_3)_3$, $Rh(NO_3)_3$, and $Eu(NO_3)_3$

They were of natural isotopic compositions instead of the separate isotopes in Table 1. However, natural Rh and Cs are composed of 100% ^{103}Rh and ^{133}Cs, respectively. The ^{149}Sm and ^{143}Nd are the dominant neutron absorbers in natural Sm and Nd. On the other hand, the Gd and Eu isotopes in Table 1 are shadowed by the other dominant absorber isotopes. Therefore, the meaning of the Gd and Eu experiments is limited for the validation purpose of the selected isotopes. The data on Gd and Eu could be used for more general benchmarking purposes. In addition, H_3BO_3 and $Er(NO_3)_3$ were selected for the experiments. Boron has a typical 1/v capture cross section so that H_3BO_3 was

utilized as a reference poison material. Erbium is used in research reactors as burnable poison and as a material to enhance the prompt negative temperature coefficient.[3] However, its nuclear data are not included in the Japanese cross section library yet. The criticality data of Er will be useful for future evaluation work.

2. Experimental Set Up

Critical Assembly Experiments were performed in an 183.2-cm-inner diameter stainless steel tank open at the upper-end as shown in Fig.1. A critical assembly contains an 18×18 square array of 320 fuel rods and parallelepiped vessel containing an aqueous solution sample. The fuel rods were arranged in a 1.956-cm-square pitch in the tank. The central 2×2 fuel rod region was replaced by the sample vessel. The approach to the critical state was performed by increasing the light water level in the core tank. A 1 cm-thick acryl grid plate was installed at the height of 58.3 cm from the active lower end of the fuel rod to maintain the geometric alignment of the fuel rods and the vessel throughout the experiment.

A plane view of the core in which reactivities of various aqueous solutions were measured is shown in Fig.2. For the case of a neutron flux distribution measurement, a bare Au wire and a Cd-covered Au wire were horizontally fixed along the east-west center line of the east half core. A plane view of the core of fuel rods, the vessel, and Au wires is shown in Fig.3.

Fuel Rods The specifications and dimensions of the fuel rods are shown in Table 2 and Fig.4. The enrichment of ^{235}U is 2.6 wt%. The 1.25 cm-diameter UO_2 pellets were clad in an aluminum tube. The active (stack) length of a fuel rod is 144.15 cm. An aluminum end plug at the lower end of the active region is 1.42 cm in diameter and 16.83 cm in length.

utilized as a reference poison material. Erbium is used in research reactors as burnable poison and as a material to enhance the prompt negative temperature coefficient.[3] However, its nuclear data are not included in the Japanese cross section library yet. The criticality data of Er will be useful for future evaluation work.

2. Experimental Set Up

Critical Assembly Experiments were performed in an 183.2-cm-inner diameter stainless steel tank open at the upper-end as shown in Fig.1. A critical assembly contains an 18×18 square array of 320 fuel rods and parallelepiped vessel containing an aqueous solution sample. The fuel rods were arranged in a 1.956-cm-square pitch in the tank. The central 2×2 fuel rod region was replaced by the sample vessel. The approach to the critical state was performed by increasing the light water level in the core tank. A 1 cm-thick acryl grid plate was installed at the height of 58.3 cm from the active lower end of the fuel rod to maintain the geometric alignment of the fuel rods and the vessel throughout the experiment.

A plane view of the core in which reactivities of various aqueous solutions were measured is shown in Fig.2. For the case of a neutron flux distribution measurement, a bare Au wire and a Cd-covered Au wire were horizontally fixed along the east-west center line of the east half core. A plane view of the core of fuel rods, the vessel, and Au wires is shown in Fig.3.

Fuel Rods The specifications and dimensions of the fuel rods are shown in Table 2 and Fig.4. The enrichment of ^{235}U is 2.6 wt%. The 1.25 cm-diameter UO_2 pellets were clad in an aluminum tube. The active (stack) length of a fuel rod is 144.15 cm. An aluminum end plug at the lower end of the active region is 1.42 cm in diameter and 16.83 cm in length.

Vessel No fuel rod was loaded in the central 2×2 rod region of the core. A parallelepiped vessel containing 2 liters of sample solution was placed in this region. The outer dimension of the vessel is 3.9cm×3.9cm×147.0cm(height). The vessel is made of 0.5-mm-thick aluminum. The level of the inner bottom surface of the vessel is 18.3mm lower than the bottom end of the active region of the fuel rod. The height of the 2 liters of solution in the vessel is 139cm.

Solution Samples In a reprocessing plant, various types of fuel solution are handled. Also, element concentration in solutions can be easily changed by experimenters. For these reasons it is felt that solutions are better physical form for a sample than solid or powder. High purity materials of over 99.9% were prepared for the samples, except for Rh for which the purity was over 99%. Given the small amount of impurity, there were no extraneous elements to be taken into account relative to the neutron absorbing effects. To make a solution sample with a specific concentration, accurately weighed material on an electronic scale was dissolved in demineralized water. After the experiments, element concentration and density of each sample were measured at the Analytical Chemistry Laboratory in JAERI. The unit of element concentration used throughout this paper, *ppm*, is equal to $\mu g/g$. Uncertainties of assay data were less than 3% for the concentration and less than 1% for the solution density.

Au wires Neutron flux distribution obtained from the experiment may provide effective data for validating nuclear data and neutron transport codes as well as criticality data. Horizontal neutron flux distributions in the core were measured with the Au wire activation method. A bare Au wire for thermal neutron distribution measurement and a Cd-covered Au wire for epithermal measurement were horizontally fixed along the east-west center

line of the east half of the core. All Au wires had a diameter of 1.0 mm. The inner and outer diameters of the cadmium tube were 1.5 mm and 2.5 mm, respectively. Vertical heights of the bare and 0.5mm-thick Cd-covered wire from the lower end of the active region of the fuel rod were 482mm and 432mm, respectively.

3. Experimental Results

3.1 Reactivity Worths of Solution Samples

The approach to the critical state was performed by increasing the light water level in the core tank. A servo-manometer indicates the water level in the tank with an accuracy of 0.05cm. When neutron detector currents on a chart recording are stable, it is decided that the core is critical. A digital reactivity meter indicates zero at that state.

The value measured by the servo-manometer was used to determine the distance between the lower end of the active region of the fuel rod and the upper surface of water (effective critical water level ; Hc). Measured Hc's for the standard core with pure water and the core with the solution sample in the vessel at the center of the core are given in the fourth column of Table 3.

The temperatures of reactor water and solutions in the vessel at critical state were measured and are listed in the third column of Table 3. Measured temperatures ranged from 9°C to 19°C. Temperature information was used for atomic number density calculations for water and solutions and to obtain the scattering laws of the moderator.

The reactivity worths of the solution samples were obtained from the difference of the critical water levels between the standard core and a core with a solution sample. Arrangement of the fuel rods and the vessel for the standard core was the same as that for a core with solution sample shown in

line of the east half of the core. All Au wires had a diameter of 1.0 mm. The inner and outer diameters of the cadmium tube were 1.5 mm and 2.5 mm, respectively. Vertical heights of the bare and 0.5mm-thick Cd-covered wire from the lower end of the active region of the fuel rod were 482mm and 432mm, respectively.

3. Experimental Results

3.1 Reactivity Worths of Solution Samples

The approach to the critical state was performed by increasing the light water level in the core tank. A servo-manometer indicates the water level in the tank with an accuracy of 0.05cm. When neutron detector currents on a chart recording are stable, it is decided that the core is critical. A digital reactivity meter indicates zero at that state.

The value measured by the servo-manometer was used to determine the distance between the lower end of the active region of the fuel rod and the upper surface of water (effective critical water level ; Hc). Measured Hc's for the standard core with pure water and the core with the solution sample in the vessel at the center of the core are given in the fourth column of Table 3.

The temperatures of reactor water and solutions in the vessel at critical state were measured and are listed in the third column of Table 3. Measured temperatures ranged from 9°C to 19°C. Temperature information was used for atomic number density calculations for water and solutions and to obtain the scattering laws of the moderator.

The reactivity worths of the solution samples were obtained from the difference of the critical water levels between the standard core and a core with a solution sample. Arrangement of the fuel rods and the vessel for the standard core was the same as that for a core with solution sample shown in

Fig.2, but the vessel was filled with pure water instead of a solution sample. In Table 3, Run Numbers 9975, 9987, 9988, 10002, 10006, 10012,10020 and 10043 are the standard cores. This method is called as the critical-water-level method. It is based on the fact that the differential water level worth, $d\rho/dH$, at a water level H is proportional to $\{1/(H+\lambda)\}^3$. By integrating $d\rho/dH$ from H_1 to H_2, the following equation is derived[4].

$$\rho[\$] = -\frac{K}{\beta_{eff}}\left\{\left(\frac{\pi}{H_1+\lambda}\right)^2 - \left(\frac{\pi}{H_2+\lambda}\right)^2\right\} , \qquad \text{Eq.(1)}$$

where,

K/β_{eff} [\$ cm^2]: reactivity-buckling conversion factor (=4309±24[5]),

β_{eff}[-]: effective delayed neutron fraction (=0.00754±0.00012[5])

λ[cm]: A sum of upper and lower extrapolation distances in vertical direction (=12.2±0.3[4]),

H_1[cm]: critical water level for the standard core,

H_2[cm]: critical water level for a core with a solution sample.

Reactivity worths calculated by Eq. (1) are shown in the fifth and sixth columns of Table 3 in the units of cent and $\Delta k/k$, and also in Fig. 5 against the atomic number density of absorber element.

3.2 Au Wire Activation Distributions

Bare and Cd-covered Au wires were irradiated under a time-integrated power of about 100 W min. After the irradiation, the wires were cut into small pieces and their gamma ray intensities were counted by a well-type NaI(Tl) detector. The intensity of a Cd-covered Au wire corresponds to the epithermal neutron flux level for which neutron energy is higher than the Cd cut-off (epi-Cd neutrons). The intensity of bare Au wire subtracted the Cd-covered one corresponds to the thermal neutron flux level for which neutron

energy is lower than the Cd cut-off (sub-Cd neutrons). Those distributions crossing the solution sample region in the horizontal direction shown in Fig. 3 were obtained for nine different solution samples and are given in Figs. 6.1 through 6.9. They were the case of pure water, 3,290ppm Sm, 64,200ppm Cs, 1,040ppm Gd, 61,500ppm Nd, 60,000ppm Rh, 6,840ppm Eu, 2,180ppm B and 12,700ppm Er. In these figures, a normalization was done so that the average sub-Cd activity in the range from 78 mm to 137 mm from the center of the core is unity.

The reactivity worths of those solution samples were derived from relationship between element concentration and reactivity listed in Table 3. Derived values for the Sm, Cs, Gd, Nd, Rh, Eu, B and Er samples were 2.98, 0.64, 2.80, 0.65, 2.18, 2.70, 2.30 and 3.26 dollars, respectively. A correlation between those values and each peak value of a sub-Cd curve at the center of the vessel, i.e. thermal neutron flux peaking, given in Figs.6.1 through 6.9 is plotted in Fig.7. Values of x- and y-coordinates in Fig.7 are not absolute but relative to those of Boron.

4. Discussion

4.1 Experimental Uncertainties

Uncertainties in the measured data are summarized in this section. As for the concentration of the neutron absorber element and the density of the solution sample, the uncertainties are less than 3% and 1%, respectively, as mentioned in Section 2. As for the reactivity, ρ, calculated by Eq. (1), the uncertainty varies owing to the difference between H_1 and H_2, i.e., the reactivity value, caused by the uncertainties in H and λ. For a small reactivity of about 10 cents, the uncertainty is about 5%, while it is about 1% for a large reactivity of about 300 cents.

energy is lower than the Cd cut-off (sub-Cd neutrons). Those distributions crossing the solution sample region in the horizontal direction shown in Fig. 3 were obtained for nine different solution samples and are given in Figs. 6.1 through 6.9. They were the case of pure water, 3,290ppm Sm, 64,200ppm Cs, 1,040ppm Gd, 61,500ppm Nd, 60,000ppm Rh, 6,840ppm Eu, 2,180ppm B and 12,700ppm Er. In these figures, a normalization was done so that the average sub-Cd activity in the range from 78 mm to 137 mm from the center of the core is unity.

The reactivity worths of those solution samples were derived from relationship between element concentration and reactivity listed in Table 3. Derived values for the Sm, Cs, Gd, Nd, Rh, Eu, B and Er samples were 2.98, 0.64, 2.80, 0.65, 2.18, 2.70, 2.30 and 3.26 dollars, respectively. A correlation between those values and each peak value of a sub-Cd curve at the center of the vessel, i.e. thermal neutron flux peaking, given in Figs.6.1 through 6.9 is plotted in Fig.7. Values of x- and y-coordinates in Fig.7 are not absolute but relative to those of Boron.

4. Discussion

4.1 Experimental Uncertainties

Uncertainties in the measured data are summarized in this section. As for the concentration of the neutron absorber element and the density of the solution sample, the uncertainties are less than 3% and 1%, respectively, as mentioned in Section 2. As for the reactivity, ρ, calculated by Eq. (1), the uncertainty varies owing to the difference between H_1 and H_2, i.e., the reactivity value, caused by the uncertainties in H and λ. For a small reactivity of about 10 cents, the uncertainty is about 5%, while it is about 1% for a large reactivity of about 300 cents.

Another point which should be noted is the difference in level between the sample solution (139 cm) and the core water at the critical state. The critical water level varied from 78 cm to 139 cm with increasing neutron poisoning of samples. In order to evaluate the reactivity effect of excess solution above the critical water level, some supplemental experiments were performed. Pure water and 400 ppm Gd were used as sample solutions for these experiments. The variation of the critical water level was measured by changing the solution level. From the experiments, it was found that the excess solution had a positive reactivity effect of less than 1.5 cents, and most of the effect came from the excess height of 5 cm. Therefore, this effect is negligible, because both of the standard and the test cores are in the same situation concerning the excess solution height.

4.2 Experimental Observations

The reactivity worths shown in Fig. 5 give some interesting observations. As for the neutron poisoning effect, Gd, Sm and Eu form the strongest group. The weakest group is formed by Nd and Cs. To the middle group belong Er and Rh. The order of neutron poisoning coincides with the order of microscopic capture cross sections for 2,200 m/sec neutrons in BNL-325.[6] However it should be pointed out that the cross section values of Er and Rh are not so much different (162 and 150 barns, respectively), and the resonance integral values of both elements are almost the same[7], therefore the discrepancy in Fig. 5 seems considerably larger than would be expected from the cross sections.

Another observation in Fig. 5 is a tendency in the reactivity effect to saturate for a high concentration of absorber element. This is mainly caused by the thermal neutron flux depression in the solution vessel, which is clearly seen in Figs. 6.2 through 6.9 compared with the standard case (pure water) in

Fig. 6.1. This phenomenon is inevitable for partially poisoned cores, and to be carefully treated in the analysis. As seen in Fig. 7, an almost linear correlation is observed between the thermal flux peak and the sample worth. This simple relation provides a useful checking point for analytical calculations.

The linear correlation is physically understood in a reactor as follows. The neutron balance in the vessel filled with solution is expressed as

$$Q = A + L , \qquad \text{Eq.(2)}$$

where Q is the slowing-down source, A the absorption rate and L the leakage rate of thermal neutrons. The sample worth ρ is almost proportional to A for a small vessel. Hence,

$$\rho \propto Q - L . \qquad \text{Eq.(3)}$$

Here, Q is almost constant as seen from the epithermal neutron flux distributions in Figs. 6.1 through 6.9. The leakage L is almost proportional to the gradient of thermal neutron flux around the vessel wall, and the gradient would be proportional to the flux peaking in the vessel because the diffusion length of the thermal neutrons is quite small in a light-water moderated system. Therefore, ρ is mainly determined by L, which suggests that the analytical calculation should be correct in the evaluation of leakage rate.

5. Conclusions

To obtain benchmark data for the principal fission product elements experimentally, the sample worths and the thermal and epithermal neutron flux distributions crossing the sample region were measured for Sm, Cs, Gd, Nd, Rh, and Eu. Er and B were also included in the measurements. Because

Fig. 6.1. This phenomenon is inevitable for partially poisoned cores, and to be carefully treated in the analysis. As seen in Fig. 7, an almost linear correlation is observed between the thermal flux peak and the sample worth. This simple relation provides a useful checking point for analytical calculations.

The linear correlation is physically understood in a reactor as follows. The neutron balance in the vessel filled with solution is expressed as

$$Q = A + L , \qquad \text{Eq.(2)}$$

where Q is the slowing-down source, A the absorption rate and L the leakage rate of thermal neutrons. The sample worth ρ is almost proportional to A for a small vessel. Hence,

$$\rho \propto Q - L . \qquad \text{Eq.(3)}$$

Here, Q is almost constant as seen from the epithermal neutron flux distributions in Figs. 6.1 through 6.9. The leakage L is almost proportional to the gradient of thermal neutron flux around the vessel wall, and the gradient would be proportional to the flux peaking in the vessel because the diffusion length of the thermal neutrons is quite small in a light-water moderated system. Therefore, ρ is mainly determined by L, which suggests that the analytical calculation should be correct in the evaluation of leakage rate.

5. Conclusions

To obtain benchmark data for the principal fission product elements experimentally, the sample worths and the thermal and epithermal neutron flux distributions crossing the sample region were measured for Sm, Cs, Gd, Nd, Rh, and Eu. Er and B were also included in the measurements. Because

such integral data for these elements have not been extensively measured before, the present data would be a good reference to validate nuclear cross section data.

In addition, some comments about the analytical calculations are given based on the experimental observations:

① There is a possibility of a misevaluation in the thermal cross section for either Rh or Er or both.

② The linear correlation between the relative sample worth and the relative thermal neutron flux peaking could be used to check the calculation performance.

③ The calculation should be sufficiently correct in the evaluation of neutron leakage rate.

Acknowledgments

The authors deeply thank the following personnel :

Yukio Toita of JAERI for assaying concentration of solution samples,
Hideyuki Hirose of JAERI for preparing the laboratory equipments for the experiments,
Kazuo Nitta of Nuclear Engineering Co., Ltd. for reactor operating support,
Takashi Horita of Chiyoda Maintenance Corporation for his data processing work, and
Tishihiro Yomamoto of JAERI for a thorough and critical review of the paper and for many suggestions.

such integral data for these elements have not been extensively measured before, the present data would be a good reference to validate nuclear cross section data.

In addition, some comments about the analytical calculations are given based on the experimental observations:

① There is a possibility of a misevaluation in the thermal cross section for either Rh or Er or both.

② The linear correlation between the relative sample worth and the relative thermal neutron flux peaking could be used to check the calculation performance.

③ The calculation should be sufficiently correct in the evaluation of neutron leakage rate.

Acknowledgments

The authors deeply thank the following personnel :

Yukio Toita of JAERI for assaying concentration of solution samples,
Hideyuki Hirose of JAERI for preparing the laboratory equipments for the experiments,
Kazuo Nitta of Nuclear Engineering Co., Ltd. for reactor operating support,
Takashi Horita of Chiyoda Maintenance Corporation for his data processing work, and
Tishihiro Yomamoto of JAERI for a thorough and critical review of the paper and for many suggestions.

References

(1) Y. Komuro, *et al.*, "Estimation of Critical Mass of Burn-up Fuel," JAERI-M 94-018 (1994).

(2) A. Santamarina, *et al.*, "Experimental Validation of Burnup Credit Calculations by Reactivity Worth Measurements in the Minerve Reactor," Proc. of the Fifth Int. Conf. on Nuclear Criticality Safety, Albuquerque, New Mexico, USA, 17-21, Sept. (1995).

(3) General Atomics, "10 MW TRIGA-LEU Fuel and Reactor Design Description," UZR-14(Rev.) (1979).

(4) H. Tsuruta, *et al.*, "Critical Sizes of Light-Water Moderated UO_2 and PuO_2-UO_2 Lattices," JAERI-1254 (1978).

(5) T. Suzaki, *et al.*, "Evaluation of β_{eff} by a Method Using Buckling Coefficient of Reactivity," 1996 Fall Mtg. of At. Ene. Soc. of Japan, A29-31, (in Japanese) (1996).

(6) S. F. Mughabghab and D. I. Garber, BNL-325, 3rd Edition(1973).

(7) S. Iijima, *et al.*, "Neutron Absorption Cross Section of Fission Products (Report of FP Working Group No.2), JAERI-1206 (1971)

Table 1 Selected fission products for burnup credit

^{99}Tc	^{95}Mo	^{103}Rh	^{133}Cs	^{143}Nd	^{145}Nd
^{147}Sm	^{149}Sm	^{150}Sm	^{152}Sm	^{153}Eu	^{155}Gd

Table 2 Specification of fuel rod

UO_2 pellet	
^{235}U enrichment [wt%]	2.596
Isotopic composition [wt%]	^{235}U : 2.596, ^{238}U : 97.404
O/M [-]	2.04
Fabrication method	Sintered
Diameter [mm]	12.50
Density [g/cm^3]	10.40
Stack length [mm]	1441.5±3
Aluminum cladding	
Inner diameter [mm]	12.65
Thickness [mm]	0.76

Table 3 Summary of reactivity measurements

Run No.	Element conc. of solution [ppm] (Element name)	Temp.* [°c]	Hc [cm]	Reactivity [¢]	Reactivity X10^{-2} [$\Delta k/k$]
9973	18x18 core	19.0/19.0	75.02	-----	-----
9974	18x18-2x2 core	19.0/19.0	77.95	-----	-----
9975	0	18.9/18.9	78.02	0	0
9976	5.02x10^2(B)	18.8/18.8	85.99	-81.4	-0.614
9977	1.00x10^3(B)	18.6/18.6	93.30	-140.4	-1.059
9978	1.53x10^3(B)	18.6/18.6	100.47	-187.5	-1.414
9979	2.06x10^3(B)	18.5/18.5	107.35	-224.8	-1.695
9987	0	17.2/17.0	78.09	0	0
9980	4.39x10^2(Sm)	17.6/16.0	85.25	-73.9	-0.557
9981	8.67x10^2(Sm)	17.5/17.3	91.69	-127.7	-0.963
9982	1.30x10^3(Sm)	17.5/17.5	97.86	-170.6	-1.286
9983	1.73x10^3(Sm)	17.5/17.5	103.96	-206.5	-1.557
9984	2.58x10^3(Sm)	17.3/17.0	115.77	-262.1	-1.976
9985	3.41x10^3(Sm)	17.3/17.0	127.01	-302.3	-2.279
9986	4.35x10^3(Sm)	17.3/17.0	138.65	-334.8	-2.525
9988	0	17.2/16.5	78.19	0	0
9989	5.15x10^2(Eu)	17.2/17.0	81.57	-36.8	-0.278
9990	1.00x10^3(Eu)	17.2/17.0	84.73	-67.9	-0.512
9992	1.51x10^3(Eu)	17.2/17.0	87.94	-96.4	-0.727
9993	2.52x10^3(Eu)	17.0/17.0	94.15	-144.6	-1.090
9994	4.07x10^3(Eu)	17.0/17.0	103.10	-200.7	-1.513
9995	6.14x10^3(Eu)	17.0/17.0	114.84	-257.0	-1.938
9996	9.42x10^3(Eu)	17.0/17.0	132.77	-318.3	-2.400

* Reactor water temp./mixture temp.

Table 3 Summary of reactivity measurements (continued)

Run No.	Element conc. of solution [ppm] (Element name)	Temp.* [°c]	Hc [cm]	Reactivity [¢]	Reactivity X10^{-2} [$\Delta k/k$]
10002	0	14.8/14.4	78.49	0	0
9997	9.91x10^{3}(Nd)	15.9/15.9	79.61	-12.6	-0.095
9998	2.01x10^{4}(Nd)	16.0/16.0	80.58	-23.0	-0.174
9999	3.03x10^{4}(Nd)	16.0/16.2	81.55	-33.2	-0.251
10003	4.06x10^{4}(Nd)	14.6/14.5	82.45	-42.4	-0.320
10004	5.08x10^{4}(Nd)	14.6/14.7	83.51	-52.8	-0.398
10005	6.49x10^{4}(Nd)	14.6/14.9	85.17	-68.5	-0.517
10006	0	13.6/13.6	78.56	0	0
10007	1.11x10^{4}(Cs)	13.7/13.6	79.65	-12.1	-0.092
10008	2.12x10^{4}(Cs)	13.8/13.7	80.70	-23.6	-0.178
10009	4.39x10^{4}(Cs)	13.9/13.7	82.76	-44.7	-0.337
10010	6.44x10^{4}(Cs)	13.2/13.4	84.71	-63.5	-0.479
10011	8.72x10^{4}(Cs)	13.5/13.5	86.67	-81.3	-0.613
10012	0	12.8/12.8	78.54	0	0
10013	5.11x10^{1}(Gd)	12.9/12.9	81.45	-31.6	-0.238
10014	1.01x10^{2}(Gd)	12.9/13.1	84.11	-58.0	-0.438
10015	2.07x10^{2}(Gd)	12.9/13.1	89.47	-105.1	-0.792
10016	4.18x10^{2}(Gd)	12.6/12.4	98.90	-172.0	-1.230
10017	6.23x10^{2}(Gd)	12.6/12.7	107.30	-218.8	-1.649
10018	8.27x10^{2}(Gd)	12.6/12.9	114.94	-253.4	-1.911
10019	1.04x10^{3}(Gd)	12.6/12.8	121.99	-280.4	-2.114
10020	0	11.1/11.2	78.71	0	0
10021	3.19x10^{3}(Er)	11.1/11.2	79.92	-13.5	-0.102
10022	1.11x10^{4}(Er)	11.1/11.3	82.90	-44.3	-0.334
10023	4.49x10^{4}(Er)	11.1/11.1	97.05	-158.3	-1.193
10024	5.77x10^{4}(Er)	10.8/10.8	101.60	-185.3	-1.397
10025	7.02x10^{4}(Er)	10.8/11.0	106.79	-214.2	-1.615
10026	9.27x10^{4}(Er)	10.8/11.0	118.36	-265.2	-1.999
10027	1.17x10^{5}(Er)	10.9/11.0	131.73	-309.4	-2.333
10043	0	9.3/8.1	78.70	0	0
10044	3.11x10^{3}(Rh)	9.2/8.4	80.25	-17.1	-0.129
10045	1.19x10^{4}(Rh)	9.2/9.3	84.68	-61.5	-0.464
10046	2.38x10^{4}(Rh)	9.2/9.9	90.68	-112.8	-0.853
10047	3.74x10^{4}(Rh)	9.1/8.8	97.13	-158.8	-1.197
10048	5.04x10^{4}(Rh)	9.2/9.3	103.82	-198.6	-1.479
10049	6.37x10^{4}(Rh)	9.3/9.7	110.90	-223.4	-1.764

* Reactor water temp./mixture temp.

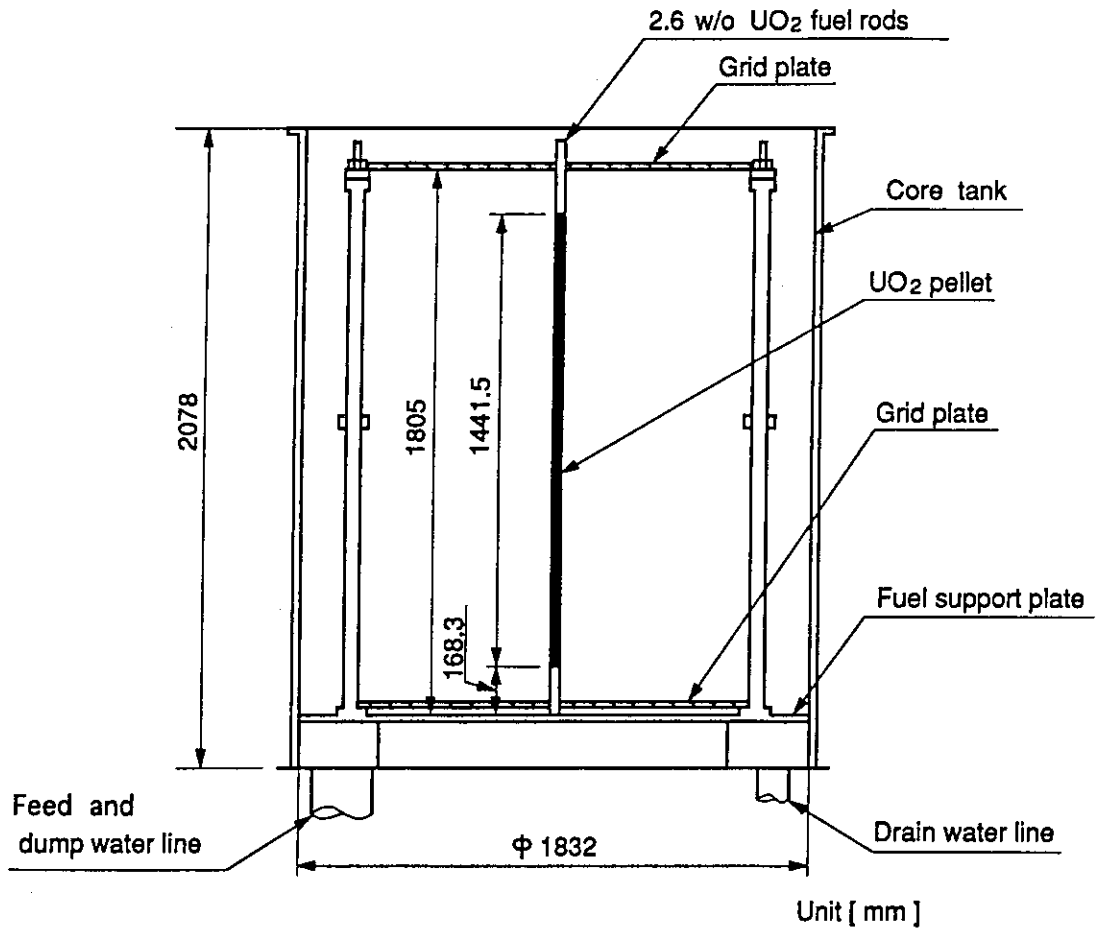

Fig. 1 Vertical cross-sectional view of TCA core tank

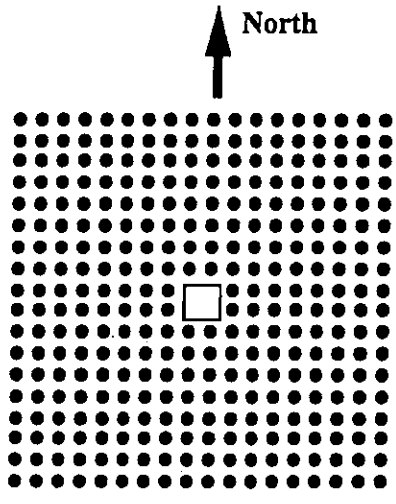

Fig. 2 Plane view of core with a solution vessel

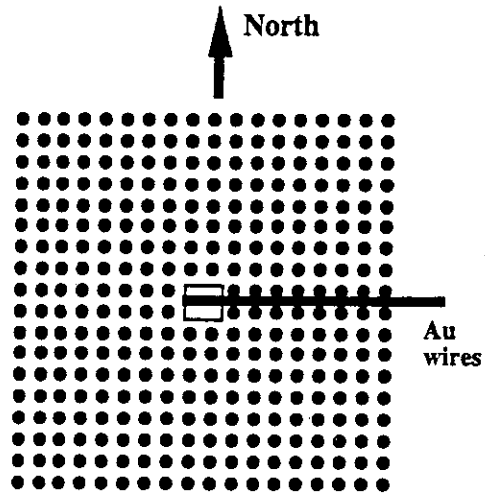

Fig. 3 Plane view of core with a solution vessel and Au wires

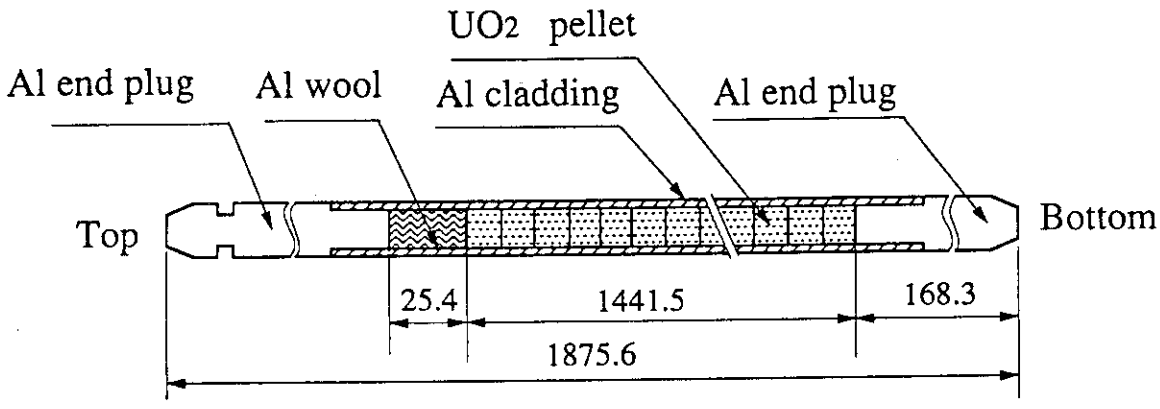

Fig. 4 2.6 wt% UO_2 fuel rod

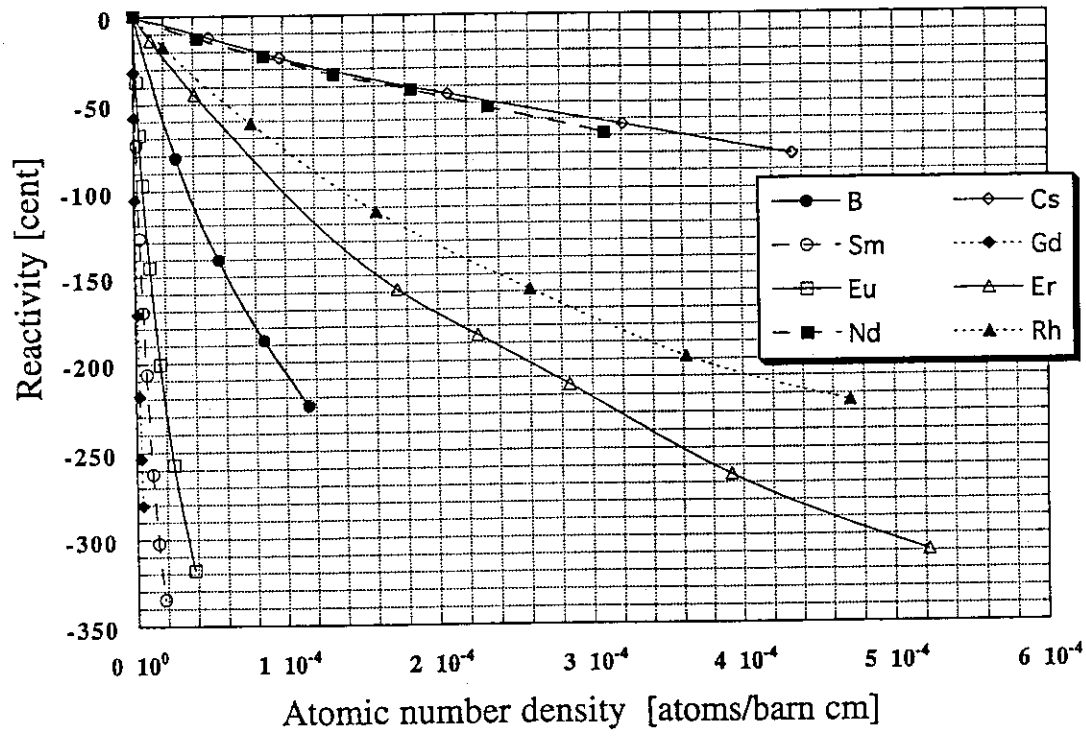

Fig. 5 Measured reactivities vs. atomic number density of absorber element

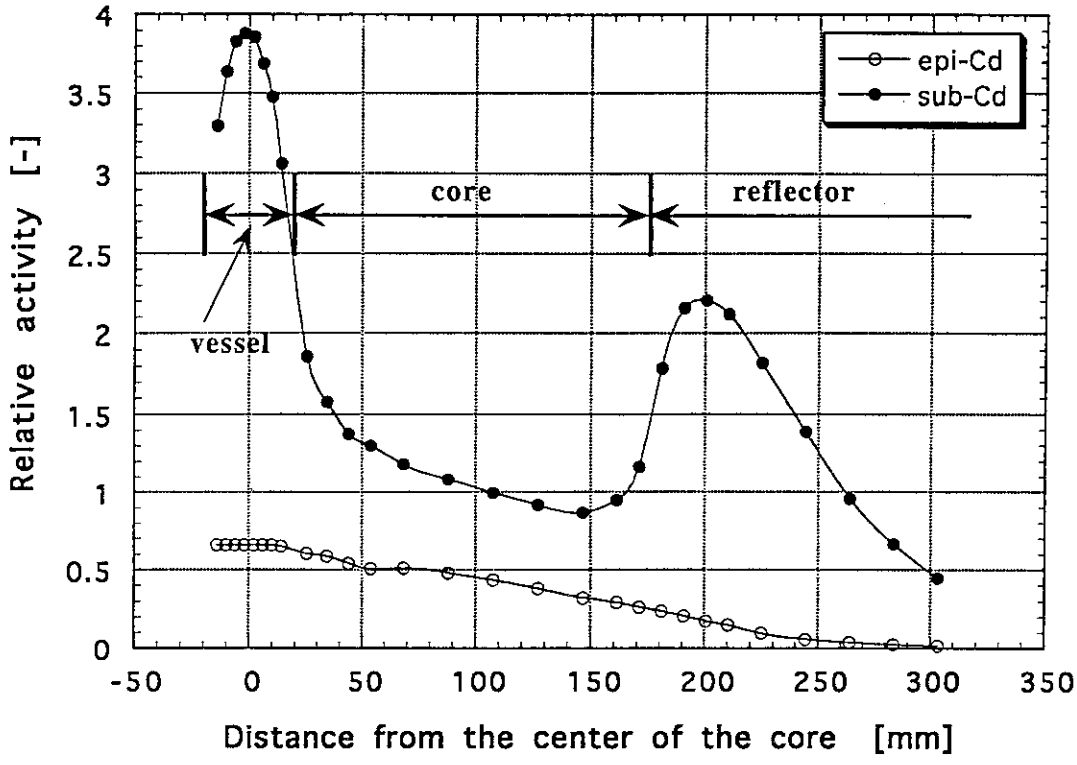

Fig. 6.1 Au wire activation traverse (H2O)

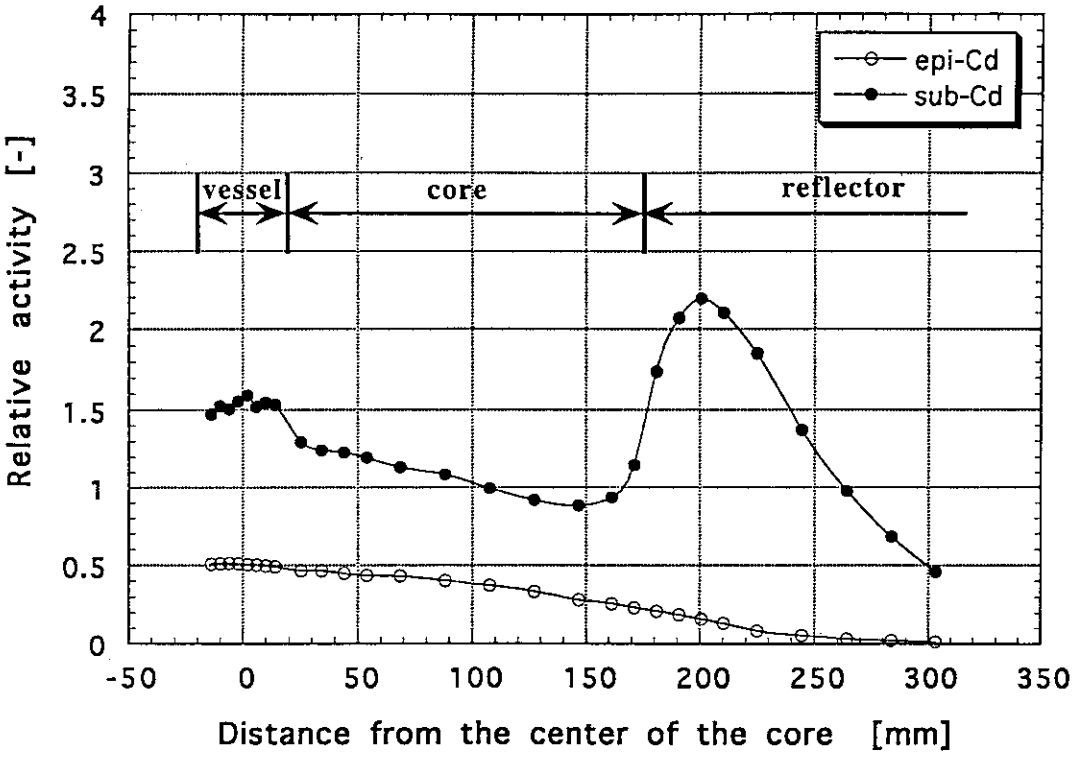

Fig. 6.2 Au wire activation traverse (3,290ppm Sm)

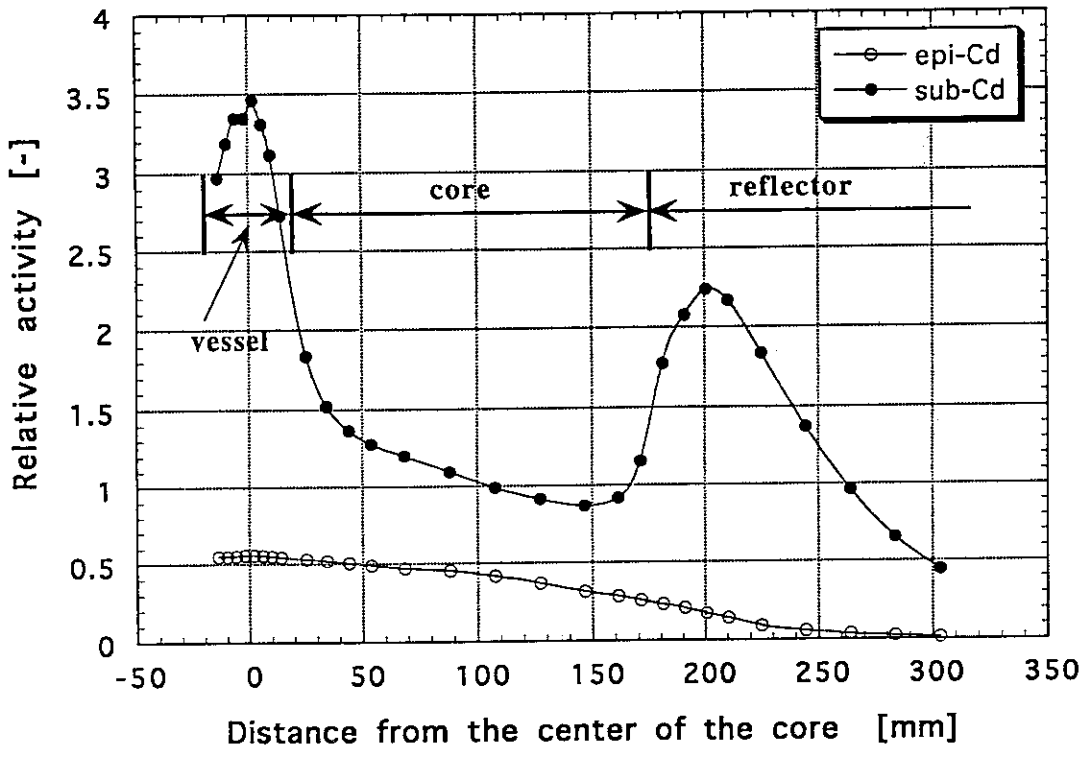

Fig. 6.3 Au wire activation traverse (64,200ppm Cs)

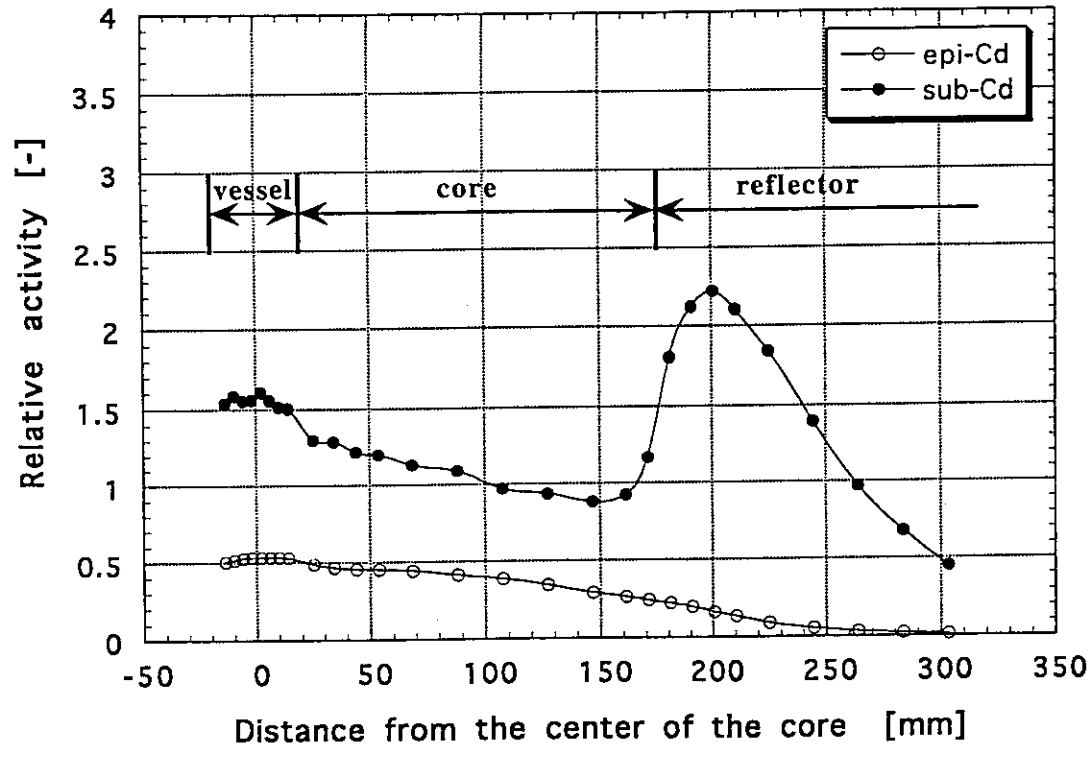

Fig. 6.4 Au wire activation traverse (1,040ppm Gd)

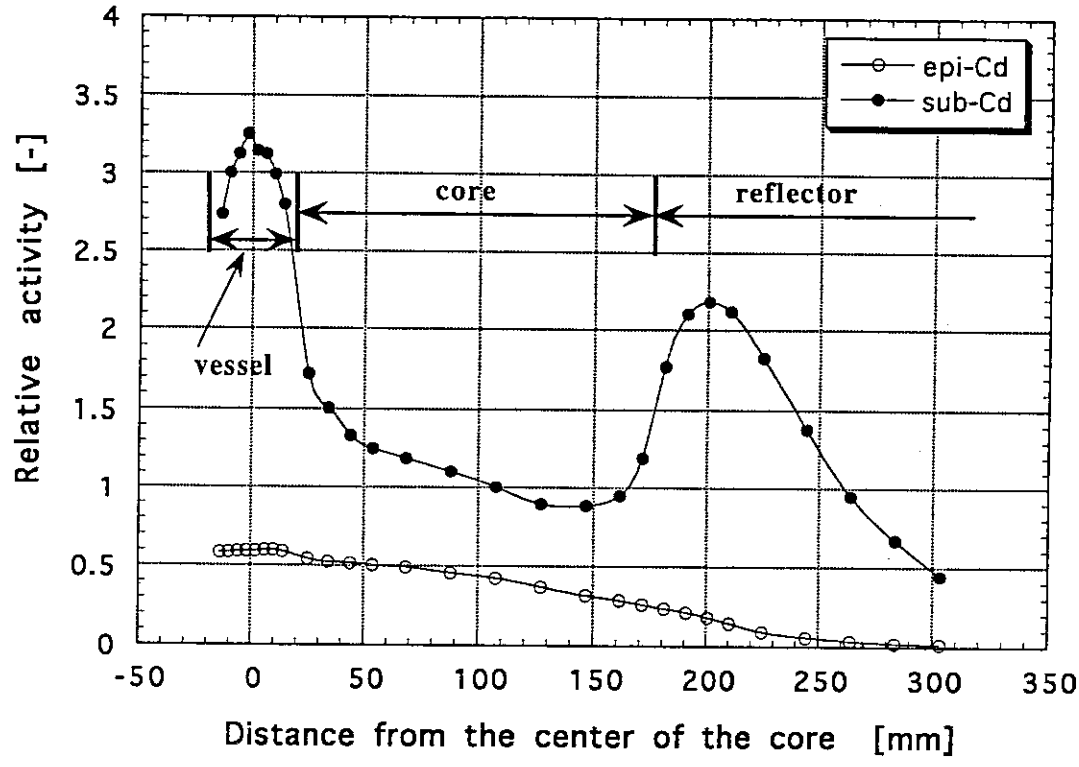

Fig. 6.5 Au wire activation traverse (61,500ppm Nd)

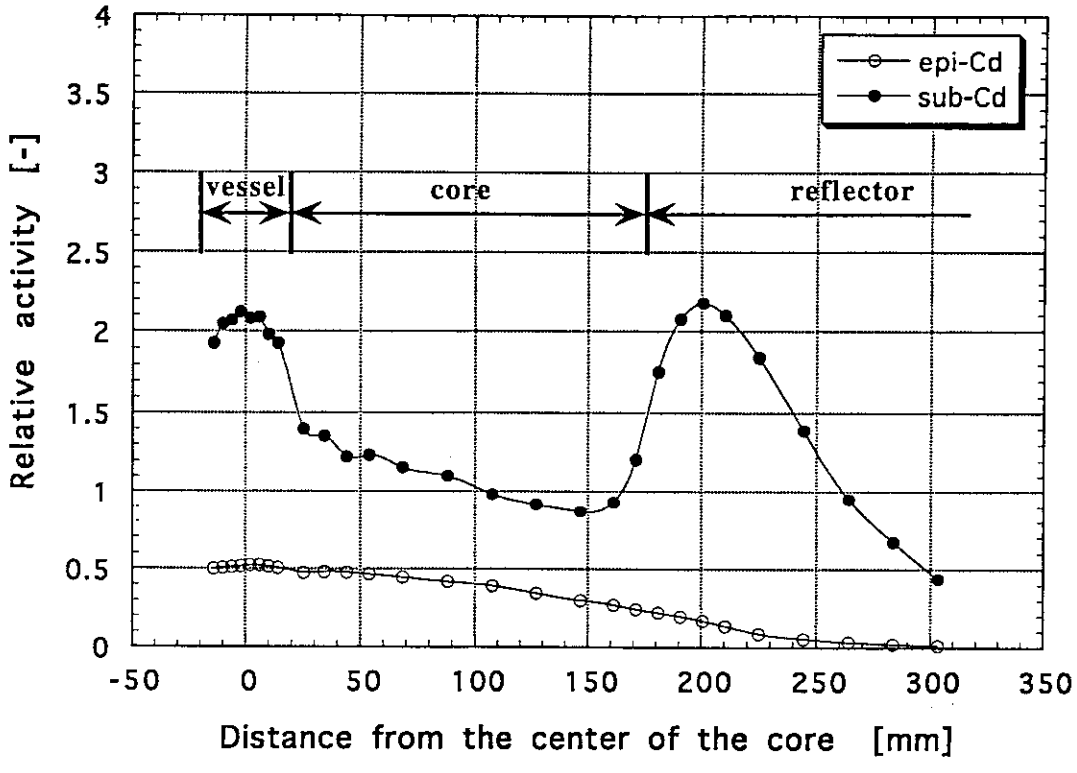

Fig. 6.6 Au wire activation traverse (60,000ppm Rh)

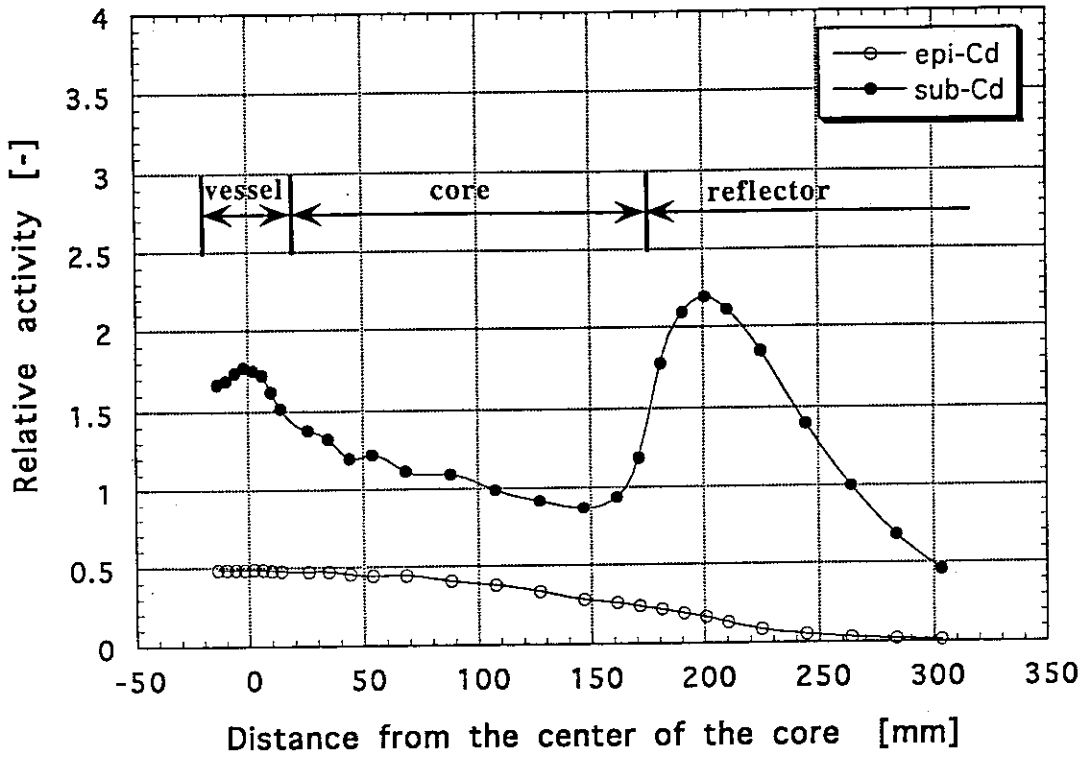

Fig. 6.7 Au wire activation traverse (6,840ppm Eu)

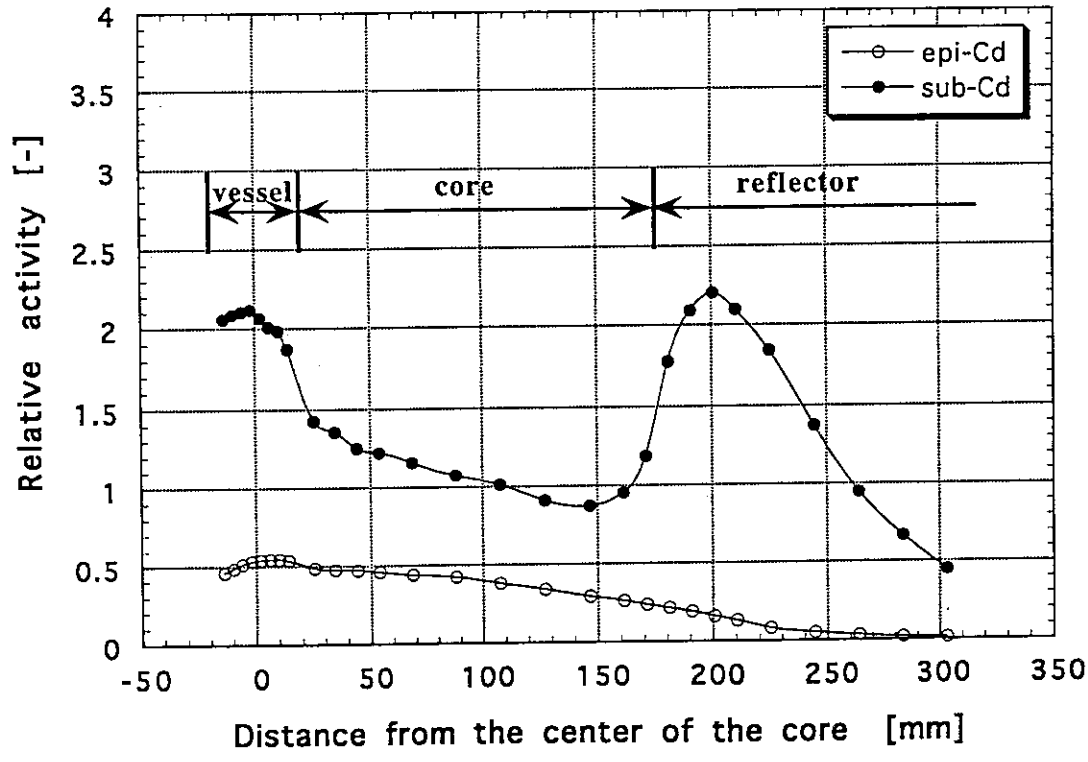

Fig. 6.8 Au wire activation traverse (2,180ppm B)

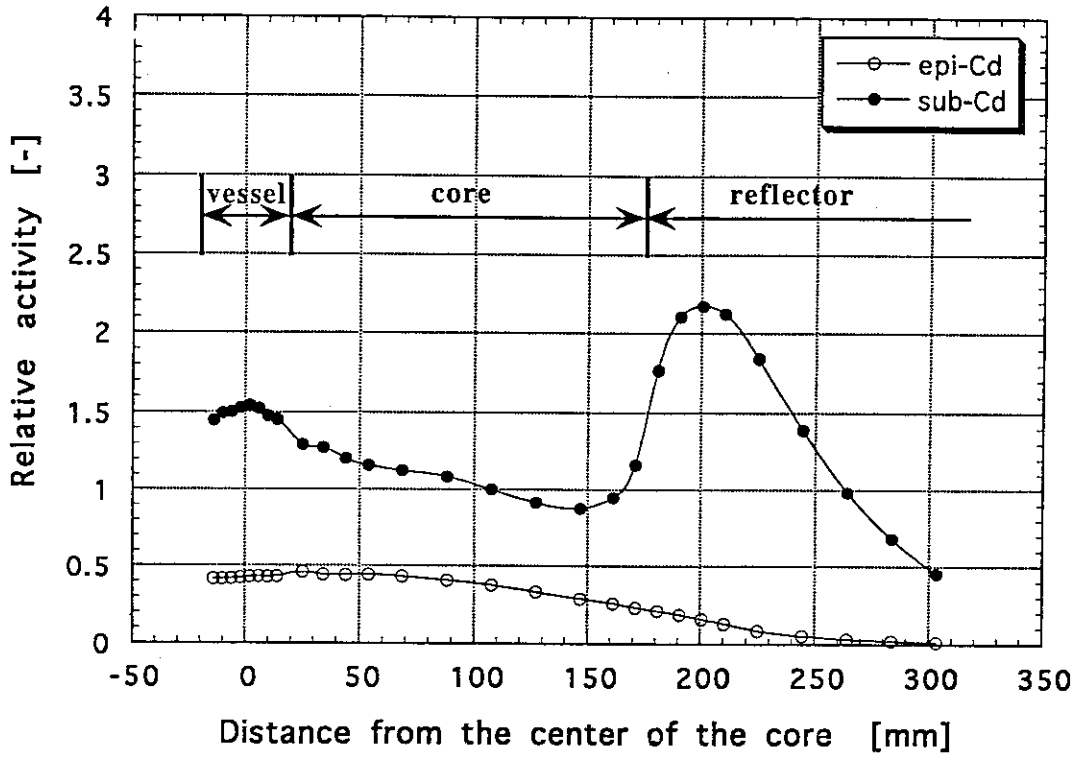

Fig. 6.9 Au wire activation traverse (127,000ppm Er)

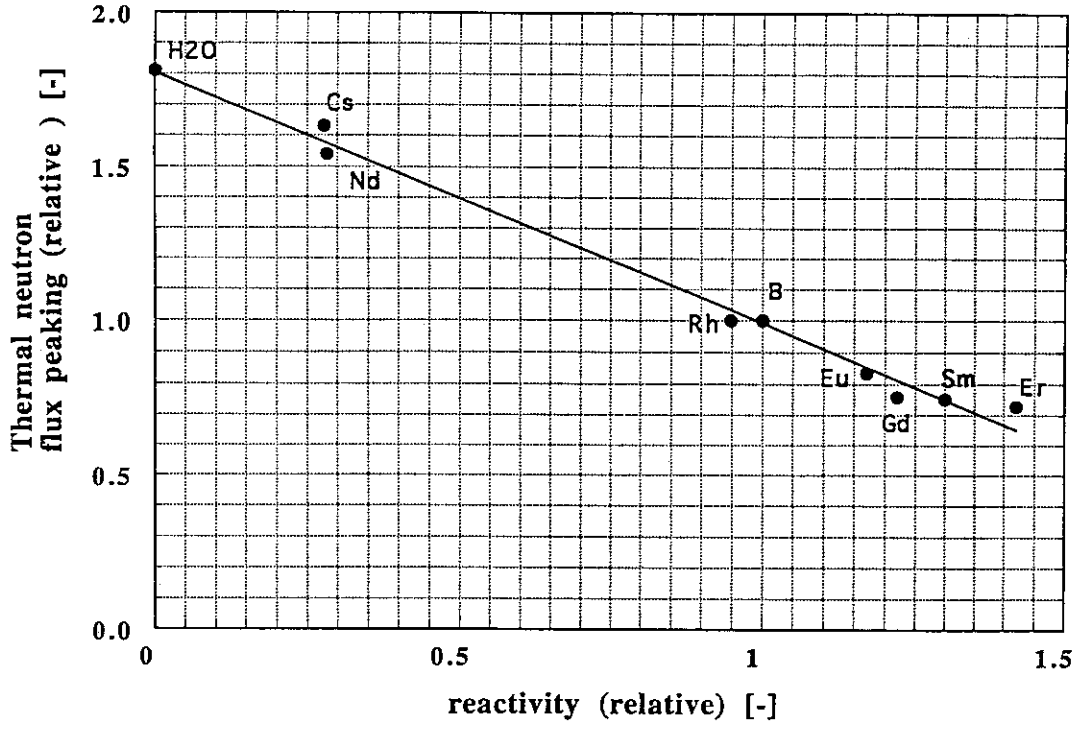

Fig. 7 Relative reactivity vs. relative thermal neutron flux peaking